Compartmentalisation of the sperm plasma membrane: a FRAP, FLIP and SPFI analysis of putative diffusion barriers on the sperm head

Peter S. James[1], Conor Hennessy[2], Torunn Berge[3] and Roy Jones[1,*]

[1]Laboratory of Molecular Signalling and [2]Bioinformatics Section, Babraham Institute, Cambridge, CB2 4AT, UK
[3]Department of Pharmacology, University of Cambridge, Cambridge, CB2 1QJ, UK
*Author for correspondence (e-mail: roy.jones@bbsrc.ac.uk)

Accepted 5 October 2004
Journal of Cell Science 117, 6485-6495 Published by The Company of Biologists 2004
doi:10.1242/jcs.01578

Summary

Spermatozoa are highly polarised cells with a compartmentalised distribution of lipids and proteins in their plasma membrane. It is not known how these compartments are stably maintained in what is essentially a fluid environment. In this investigation we have examined the hypothesis that intramembranous diffusion barriers selectively retain some components within compartments, while allowing free passage of others. A fluorescence loss in photobleaching analysis of the behaviour of the lipid reporter probe 1,1′-dihexadecyl-3,3,3′3′-tetramethyindocarbocyanine ($DiIC_{16}$) on the head of boar spermatozoa revealed that it was freely diffusing between all three compartments (anterior acrosome, equatorial segment and postacrosome). Spermatozoa also contained rapidly diffusing particles of $DiIC_{16}$ over the anterior acrosome and equatorial segment. These particles, ~200 nm in diameter, were tracked in real time and their trajectories analysed by mean square displacement. Particle diffusion was essentially random over the anterior acrosome and equatorial segment but showed a periodicity in jump sizes and diffusion coefficients suggestive of microheterogeneities. Particles did not exchange between the equatorial segment and postacrosome, indicating a barrier at the junction between these two compartments. No barrier was detected between the equatorial segment and anterior acrosome. A model is proposed in which a molecular 'filter' is present at the equatorial segment-postacrosomal boundary that allows free passage of single molecules but not molecular complexes. Passage of heterogeneous complexes, such as lipid rafts, requires disassembly and reassembly on either side of the filter.

Key words: Compartmentalisation, Sperm plasma membrane, Diffusion barriers, Equatorial segment, Lipid rafts

Introduction

The lateral distribution of lipids and proteins in cell membranes is known to be highly asymmetric (Edidin, 1993; Jacobson et al., 1995; Vereb et al., 2003). Elucidating how these heterogeneities are generated and maintained over relatively large distances against the randomising forces of diffusion is central to understanding many of the processes involved in cell differentiation and establishment of polarity.

Uncontrolled mixing of membrane components is thought to be prevented by several complementary processes, the best known of which are interaction with the cytoskeleton, spontaneous self-association, selective internalisation and confinement behind diffusion barriers (Gumbiner and Louvard, 1985). Diffusion barriers have long been implicated in the asymmetric distribution of surface antigens, such as between the cell body and axon in neurons (Kobayashi et al., 1992), the inner and outer segments of retinal rod cells (Peters et al., 1983) and the apical and basolateral membranes in epithelial cells (Rodriguez-Boulan and Nelson, 1989), and are thought to be largely responsible for creating micrometer-sized macrodomains. Frequently, they have a physical basis in the form of electron-dense structures within the membrane, e.g. zona occludens between epithelial cells (Dragsten et al., 1981). However, confinement zones also exist at the nanometer scale. These were first suggested by low recovery rates during fluorescence photobleaching (FRAP) experiments and later demonstrated directly using laser tweezers to drag 40 nm gold particles across the cell surface (Edidin, 2003; Vereb et al., 2003). Recent work by Kusumi and co-workers (Fujiwara et al., 2002; Murase et al., 2004) using single particle tracking at very high video speeds have refined this idea into the 'picket and fence model', in which proteins and lipids are confined temporarily within 200-300 nm diameter compartments and effect long-range diffusion by 'jumping' between compartments. It is not altogether clear at present how the temporary confinement model accommodates lipid rafts, which are envisaged as dynamic structures varying in size from a few molecules to ~50 nm in diameter and are rich in cholesterol, glycosphingolipids and GPI-anchored proteins (Edidin, 2003). At all levels of scale, it seems that membrane compartments are influenced by the cytoskeleton, thereby affording a means of transducing signals from the cytoplasm to the cell surface and vice versa.

The mammalian spermatozoon is an example of a polarised cell with a highly compartmentalised plasma membrane (Holt, 1984; Cardullo and Wolfe, 1990). During differentiation in the

testis from a round spermatid into an elongated spermatozoon, the plasma membrane becomes subdivided into three compartments overlying the head (known as the anterior acrosome, equatorial segment and postacrosome) and two on the tail (the midpiece and principal piece), each with its own complement of proteins and lipids. For the most part, these compartments appear relatively stable, although there is evidence for exchange of membrane components between them in response to external stimuli (e.g. Ca^{2+}), usually in the form of polarised migration of GPI-anchored glycoproteins and glycosphingolipids (Cowan et al., 1987; Jones et al., 1990; Gadella et al., 1994; Hunnicutt et al., 1997; Shadan et al., 2004). This lateral reorganisation of membrane components during developmental processes such as maturation and capacitation is crucial for spermatozoa, as it constitutes a fine control mechanism to ensure that key molecules are in the correct location at the correct time to mediate fertilisation.

As mature spermatozoa are transcriptionally inactive and contain very little cytoplasm, many of the mechanisms found in somatic cells for maintaining lateral asymmetry (e.g. polarised trafficking from the Golgi, selective internalisation) are inconsequential or non-existent. Much interest, therefore, has focused on the role of diffusion barriers for maintaining membrane compartmentalisation. Conventional FRAP analysis has added weight to this concept by demonstrating five- to tenfold differences in diffusion coefficients for lipids and proteins between compartments (Cowan et al., 1987; Cowan et al., 1991; Cowan et al., 2001; Wolf, 1995; Ladha et al., 1997; Wolfe et al., 1998). Explanations for these disparities, however, have not been forthcoming. A limitation of FRAP is that it measures the diffusion of tens of thousands of molecules and is not informative about complex phenomena such as non-ideal mixing of lipids or the dynamics of raft formation. To investigate the presence of diffusion barriers in sperm tails we devised a video-FRAP procedure to measure the directionality of recovery of the lipid reporter probe $DiIC_{12}$ following bleaching of a ~2.5 μm diameter spot adjacent to two electron-dense structures in the membrane known as the posterior ring (at the junction of the head and midpiece) and annulus (between the midpiece and principal piece) (Mackie et al., 2001). This was possible because the tail could be regarded essentially as a cylinder showing one-dimensional diffusion. Neither the posterior ring nor annulus prevented diffusion of $DiIC_{12}$ molecules between compartments.

Potential diffusion barriers are also present on the sperm head at the junction between the postacrosome and equatorial segment and between the equatorial segment and anterior acrosome. The three regions so enclosed have different antigenic profiles (Primakoff and Myles, 1983) and different surface topographies as viewed by atomic force microscopy (Ellis et al., 2002). Unfortunately, directional recovery analysis cannot be applied to the sperm head, which has to be regarded as a planar surface in which diffusion is two-dimensional. To circumvent this problem, we have applied techniques of fluorescence loss in photobleaching (Van Drogen and Peter, 2004) in combination with single particle fluorescence imaging (Anderson et al., 1992) to investigate putative diffusion barriers on the sperm head. Our hypothesis predicts that these barriers behave as selective 'filters', to account for the confinement of specific antigens within them while allowing free passage of others. Results suggest that while single lipid molecules are freely diffusing throughout the head plasma membrane, large molecular complexes are unable to cross the boundary between the postacrosome and equatorial segment. We propose a model that involves disassembly-reassembly of molecular complexes on either side of putative membrane barriers.

Materials and Methods

Materials

All routine chemicals were of the highest purity available commercially and were purchased from Merck-Eurolab (Lutterworth, UK) or Sigma-Aldrich (Poole, UK). Fluorescent lipids (1,1′-didoecyl-3,3,3′,3′-tetramethylindocarbocyanine perchlorate ($DiIC_{12}$) and 1,1′-dihexadecyl-3,3,3′,3′-tetramethylindocarbocyanine perchlorate ($DiIC_{16}$) were obtained from Molecular Probes (Leiden, The Netherlands). Fatty acid-free bovine serum albumin (BSA) was supplied by Sigma-Aldrich. Ejaculated spermatozoa were obtained fresh from boars maintained at the Babraham Institute or purchased pre-diluted in a commercial extender from JSR Newsham Ltd (Thorpe Willoughby, UK). All procedures involving animals were carried out within UK Home Office approved guidelines. Testicular, caput and cauda epididymidal spermatozoa were collected from tissues within 1-2 hours after slaughter of mature boars. All spermatozoa were diluted in HEPES buffered TALP medium (Parrish et al., 1988) minus Ca^{2+} and HCO_3^- and washed once by centrifugation through 35:70% Percoll in HEPES/TALP. The live sperm fraction at the bottom of the gradient was resuspended in HEPES/TALP and adjusted to ~10^7 cells/ml.

Preparation of BSA-$DiIC_{12}$ and BSA-$DiIC_{16}$

Stock solutions of $DiIC_{12}$ (2.5 mmol/l) and DiC_{16} (2.8 mmol/l) were prepared in 100% ethanol and stored at –20°C under nitrogen. For conjugation of DiI probes to BSA, the procedure of Mukherjee et al. (Mukherjee et al., 1999) was followed. Briefly, working solutions of 0.75 μmol DiC_{16} and 0.075 μmol $DiIC_{12}$ were prepared by dilution in ethanol from which 400 μl aliquots were removed and added to 4 ml of 3.3 mg/ml BSA in phosphate buffered saline (PBS) while mixing continuously. Solutions were dialysed against several changes of PBS at 4°C to remove the ethanol and the particulate suspension that formed centrifuged at 100,000 ***g*** for 20 minutes at 4°C. Supernatants were passed through Sepharose G-25 (PD-10) columns equilibrated in PBS, the BSA-DiI fractions sterilized by passage through 0.2 μm filters and stored at –20°C.

Labelling of spermatozoa with $DiIC_{12}$ and $DiIC_{16}$

Spermatozoa were labelled with $DiIC_{12}$ or $DiIC_{16}$ either in 1% ethanol (Wolfe et al., 1998) or by back-exchange from a BSA carrier. Probes were diluted to 20 μmol in 2% ethanol, mixed with an equal volume of spermatozoa in HEPES/TALP and incubated for 15 minutes at 38°C. Spermatozoa were then diluted with 0.5 ml of medium, washed twice by centrifugation (450 ***g*** for 10 minutes) and resuspended to 50 μl in the same medium. For back-exchange labelling, spermatozoa (100 μl in HEPES/TALP medium) were mixed with 10 μl of BSA-$DiIC_{16}$ or 2 μl of BSA-$DiIC_{12}$, incubated for 10 minutes at 38°C and washed twice by centrifugation with 0.5 ml of HEPES/TALP. After resuspension in the same medium, spermatozoa were viewed at intervals between 1 and 6 hours incubation at room temperature.

Microscopy

Spermatozoa stained with $DiIC_{12}$ or $DiIC_{16}$ were drawn by capillary action into glass microslides (VD/5005-050; Camlab, Over, UK) and viewed using epifluorescence microscopy, atomic force microscopy, fluorescence photobleaching, fluorescence loss in photobleaching, and single particle fluorescence imaging.

Epifluorescence microscopy

The epifluorescence microscopy was performed using a Zeiss Axiophot photomicroscope fitted with a 100 W mercury vapour lamp and a X100 phase objective with oil immersion. Colour photographs were taken using a Diagnostic RT colour camera utilizing SPOTRT software 3.0 (Diagnostic Instruments, Sterling Heights, MI, USA).

Atomic force microscopy

For the atomic force microscopy (AFM), 50 µl of spermatozoa (labelled and unlabelled) in TALP medium were applied as drops to clean glass coverslips and incubated for 20 minutes. Adhered spermatozoa were rinsed briefly with MilliQ water and air dried. AFM images were taken using a Multimode Atomic Force Microscope with a Nanoscope IIIa controller (DI Veeco, Santa Barbara, CA) as described previously (Ellis et al., 2002).

Fluorescence photobleaching and fluorescence loss in photobleaching

Fluorescence photobleaching (FRAP) was performed using a custom-built apparatus and dedicated software as described previously (Ladha et al., 1997; Mackie et al., 2001). For fluorescence loss in photobleaching (FLIP) analysis (van Drogen and Peter, 2004), the same apparatus was used, except the pinhole was enlarged to give a bleach beam of ~2.0 µm diameter, which was positioned either over the anterior tip of the acrosome or on the postacrosome adjacent to the neck region. 'Before' images were captured, the UV illumination closed and six to eight bleaches carried out in succession with 6 second recovery periods. The UV shutter was then opened and 'after' images captured on a Sony Ultrapix FSI camera using Perkin Elmer UltraVIEW software at a frame rate of ten frames/second. Line intensity profiles were analysed using the multiplekymograph plugin in Image J (http://rsb.info.nih.gov/ij/).

Single particle fluorescence imaging

For single particle fluorescence imaging (SPFI), microslides containing labelled spermatozoa were viewed with a Noran OZ confocal laser scanning microscope equipped with Intervision software. Samples were illuminated with the 514 nm emission wavelength from an Argon air-cooled laser and imaged with a ×60 objective lens (numerical aperture 1.4) using a digital zoom (×2) camera with 220×230 pixels resolution. Successive images were collected at 30 frames/second for up to 1 minute, saved in SGI format and analysed using Image J (NIH, Bethesda, MD).

Particle tracking analysis

An algorithm with the following components was used to track moving particles on the sperm head. Background diffusion intensity of individual pixels over time was estimated using a Kalman Filter (1960). It was initialised by running the filter with a relatively low Kalman Gain over the foremost frames and then proceeded in unison with the tracking algorithm below, adding each frame with a stricter gain. This not only gave a forecast of the background intensity of each pixel (b^f_{ij}) (ij, image coordinates; f, frame no.) in a particular frame but also gauged the variance in its intensity (v^f_{ij}) over time. Particle location was then accentuated using the following filter:

$$e^f_{ij} = -\Sigma_{uv} \mathrm{LoG}(i-u,i-v) \times \{p^f_{uv} - [b^f_{uv} + \mathrm{sqrt}(v^f_{uv})]\} , \quad (1)$$

where LoG=Laplacian of Gaussian kernel:

$$\mathrm{LoG}(x,y) = -1 / (\pi\sigma^4) \, [1-(x^2+y^2)/2\sigma^2] \exp[-(x^2+y^2)/2\sigma^2] . \quad (2)$$

This nullifies stationary objects, but the tracking of such cases was considered a trivial task. To avoid this computationally expensive operation being applied to each pixel in all frames, tracking was done using a Particle Filter approach. In each frame the target location was estimated from a weighted sum of independent particles. The a priori location of particles in the current frame was postulated from Brownian motion of particles from the previous frame. The above filter was then used to weight these hypothesised positions to give the a posteriori estimate of target location. Particles were re-sampled regularly to remove redundant cases. An advantage of this approach, other than efficiency, is robustness. Thanks to the weighted re-sampling, particle locations were localised for strong hits and dispersed over an expanding search area when only weak hits were prevalent. Confidence about the estimate of location was thus indicated by the variance of that estimate. Problematic frames were subsequently apparent (in fact, in the end-user interface confidence is represented by a target box around the estimated position, which expands as confidence decreases).

Occasional spermatozoa were found with multiple particles moving in close proximity. A possible solution to this would be to simply run a single tracker per target. A probable result would have been all trackers eventually gravitating towards the strongest hit particle. Conversely, the result could have been all targets being tracked by a division of the particles of a single tracker and the resulting estimation being a midpoint of all targets. The Brownian motion of the particles means that multiple targets cannot be distinguished over time using estimated velocity state as would be the case for missile tracking. To overcome this, all moving particles were tracked simultaneously with an exclusion function penalising particles from separate trackers that came too close. This kept each tracker always focused towards its own target. It was found that the re-sampling step of Khan et al. (Khan et al., 2004) was very efficient without requiring extra particles per target as would be the case for a combined state particle filter. A user interface containing the above algorithm was created as a plug-in to the Image J software package available from NIH (Bethesda, USA).

Calculation of particle jump size, diffusion coefficient and mean square displacement

Following image analysis of the tracks provided by Image J, the data was downloaded into Microsoft Excel. From the magnification of the confocal images each pixel was estimated to be 60 nm in diameter. The mean square displacement (MSD) was calculated from the following equation:

$$\mathrm{MSD}(t) = \frac{1}{F-1} \sum_{f=2}^{F} \left| \vec{x}_f - \vec{x}_{f-1} \right|^2 , \quad (3)$$

where t=time between frames, x_f=coordinates in frame f, and F= number of frames.

The diffusion coefficient for the $DiIC_{16}$ particles was calculated over discrete time periods, utilising the equation:

$$D = \mathrm{msd}/4t . \quad (4)$$

Mean data for 300 ms time periods were plotted against time.

Results

FRAP analysis of $DiIC_{12}$ and $DiIC_{16}$ diffusion in the plasma membrane of live boar spermatozoa

Live boar spermatozoa stained with $DiIC_{12}$ in 1% ethanol showed uniform fluorescence over their entire surface, indicating incorporation of the lipid into all regions of the plasma membrane. By contrast, dead or damaged spermatozoa stained more strongly on specific regions, usually the acrosome and midpiece, reflecting rupture of the plasma membrane and staining of underlying organelles (Ladha et al., 1997). FRAP analysis of live cells gave the following diffusion coefficients (D): acrosome, $72.3\pm6.6\times10^{-9}$ cm^2/second; postacrosome, $48.2\pm9.8\times10^{-9}$ cm^2/second; midpiece region, $9.1\pm1.6\times10^{-9}$ cm^2/second; principal piece region, $22.7\pm4.8\times10^{-9}$ cm^2/second;

figures are means±s.e.m., *n*=35 spermatozoa. These D values follow the same general pattern obtained earlier with the 5-(N-octadecanoyl)aminofluorescein reporter (Wolfe et al., 1998), i.e. 3-5 times faster diffusion on the acrosomal region than on the tail. By contrast, when $DiIC_{16}$ was dissolved in 1% ethanol, live spermatozoa were either unstained or showed a few small particles of dye (<0.5 μm diameter) adhering to the surface membrane. Unlike $DiIC_{12}$, $DiIC_{16}$ is poorly soluble in aqueous media (even in the presence of 1% ethanol) and sticks non-specifically to the walls of plastic Eppendorf tubes. The insolubility of DiI probes increases with chain length so that with $DiIC_{18}$ no spermatozoa (live or dead) incorporated the reporter probe.

To overcome the problems of solubility with longer chain DiI probes, we utilized back-exchange from BSA with greater success. Spermatozoa incubated with BSA-$DiIC_{12}$ stained similarly to those using $DiIC_{12}$ in 1% ethanol, whereas with BSA-$DiIC_{16}$ several different labelling patterns were obtained. The predominant pattern (73±9%; *n*=5 experiments, 100 spermatozoa/experiment) consisted of spermatozoa showing uniform fluorescence over the entire surface, with several small strongly fluorescent particles adhering to the head region (Fig. 1A,B,C and upper sperm in D). The position of the particles varied and they were rarely found on the tail. These spermatozoa were frequently motile. FRAP analysis of $DiIC_{16}$-labelled spermatozoa with <3 attached particles gave the following D values: acrosome, $49.5\pm17.5\times10^{-9}$ cm^2/second; postacrosome, $44.9\pm18.3\times10^{-9}$ cm^2/second; midpiece, $8.2\pm1.9\times10^{-9}$ cm^2/second; these are means±s.e.m., *n*=27 spermatozoa. Other labelling patterns included spermatozoa heavily encrusted with >20 fluorescent particles over the acrosome (16±4%, 100 spermatozoa/experiment, *n*=5 experiments; lower sperm in Fig. 1D) and spermatozoa with very intense fluorescence over the whole head and tail (11±2%, *n*=5 experiments). Spermatozoa in the last two categories were always immotile and were considered to be dead or damaged cells.

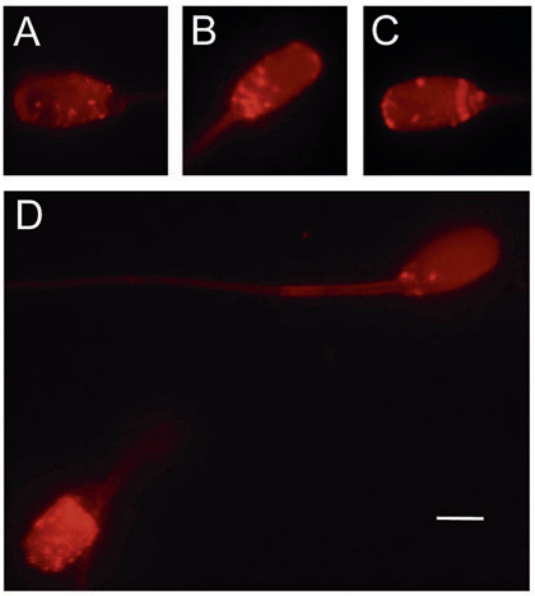

Fig. 1. Boar spermatozoa stained with $DiIC_{16}$ by back-exchange from BSA-$DiIC_{16}$. Live spermatozoa (A,B,C and upper sperm in D) showed uniform fluorescence throughout the plasma membrane with varying numbers of small strongly fluorescent particles attached to the head region. Dead sperm (lower sperm in D) were typically heavily stained on the acrosomal region (see Fig. 3 for definitions of compartments within the sperm head region). Bar, 4 μm.

FLIP analysis of $DiIC_{16}$ diffusion across the equatorial segment/postacrosomal boundary

Because the $DiIC_{16}$ incorporated into live spermatozoa could be back-exchanged with fatty-acid-free BSA, it is presumed to have intercolated into the outer leaflet of the plasma membrane. Aside from the particles (see later), it is also presumed that the incorporated $DiIC_{16}$ diffuses as single molecules. If so, and they are freely exchangeable throughout the sperm head plasma membrane, then repeated exposure of a small area to a laser beam near the anterior tip of the acrosome should cause the whole head to gradually decrease in fluorescence intensity. If, however, a diffusion barrier is present at the junction between the postacrosome and equatorial segment, then the bleached $DiIC_{16}$ on the acrosome would not be replenished and the postacrosome would remain preferentially labelled. This is the basis of FLIP analysis. The results of these experiments are shown in Fig. 2. Repeated photobleaching (6-8 times) of an area ~2.0 μm in diameter on the anterior tip of the acrosome caused a progressive decrease in fluorescence intensity over the entire sperm head, indicating recruitment of unbleached $DiIC_{16}$ molecules from the postacrosome to the acrosome. This was confirmed by line profile analysis, which showed no difference in fluorescence intensity between the postacrosme and equatorial segment; recoveries were typically ~90%. Similarly, FLIP with the bleach spot positioned on the postacrosome showed replenishment of bleached with unbleached $DiIC_{16}$ from the direction of the acrosome. Thus, single $DiIC_{16}$ molecules are freely diffusing in both the anterior and posterior directions across the boundary between the equatorial segment and postacrosome.

The above FLIP analysis was repeated on immature testicular spermatozoa, which contain more saturated lipids than ejaculated cells. Results (not shown) were essentially the same as those given above, indicating that maturation of spermatozoa in the epididymis does not have any measurable effect on exchange of $DiIC_{16}$ molecules between different membrane compartments.

Presence of mobile $DiIC_{16}$ particles on the sperm head

A feature of the $DiIC_{16}$-labelled live spermatozoa was the presence of fluorescent particles that diffused rapidly within the confines of the acrosomal region of the sperm head. The number of these particles varied from 1 to 6 per sperm and their size ranged from ~100 to ~400 nm in diameter. They never moved beyond the boundary of the sperm head and remained on one face only, i.e. they did not cross over the acute angle at the edge of the head. Mobile particles on the postacrosome were very rare. The proportion of spermatozoa with mobile particles on the acrosomal plasma membrane increased from ~5% at 0 min to ~28% after 4 hours' incubation at room temperature, although the latter value varied between individual boars (range 16-52%). In this respect, the most consistent results were obtained using the commercial semen,

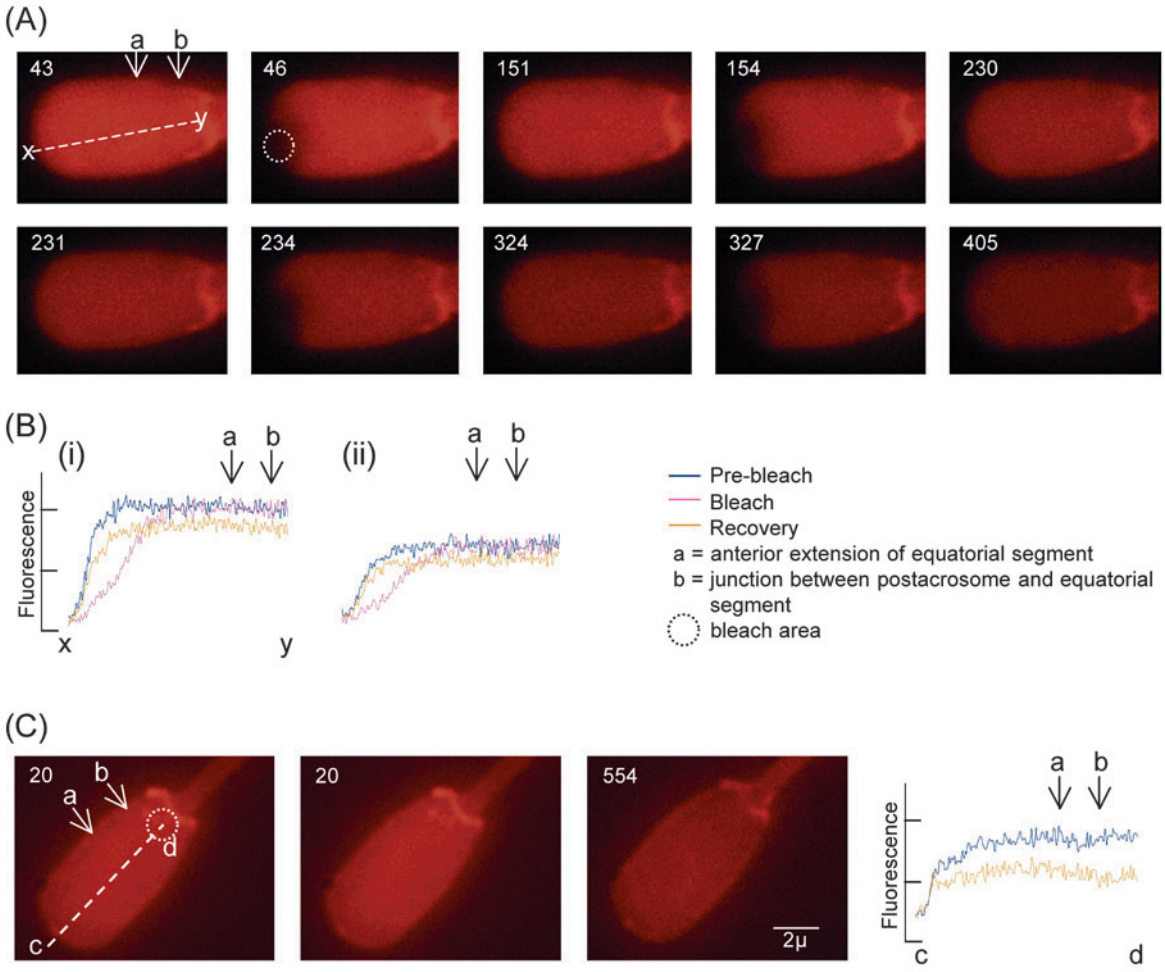

Fig. 2. FLIP analysis of $DiIC_{16}$ diffusion in the plasma membrane overlying the sperm head. (A) Separate frames from a video sequence to illustrate repeated photobleaching of a ~2.0 μm diameter area located at the tip of the anterior acrosome (broken circle, frame 46). Only four out of the six bleaches are shown (bleaches were in frames 45, 153, 233 and 326). With each successive bleach, the intensity of fluorescence over the whole head declines uniformly. (B) (i) line-profile analysis of fluorescence intensity along the x-y axis shown in A in the pre-bleach state (frame 43), immediately post-bleach (frame 46), and after 3 seconds' recovery (frame 151); (ii) same as in (i) except after four successive bleaches (recovery frame 405). Arrows at 'a' and 'b' mark the anterior and posterior positions of the equatorial segment. Note that fluorescence intensity is similar across the equatorial segment-postacrosome boundary. (C) Similar to A except the bleach beam is located over the postacrosome (broken circle in pre-bleach frame 20). There was no difference in fluorescence intensity along the c-d axis after six successive bleaches (frame 554), indicating free diffusion of the lipid between surface compartments. Bar, 2 μm.

which is from boars selected for high fertility. This phenomenon, however, was not investigated further.

The presence of mobile particles was also related to the degree of maturation of the spermatozoon. Testicular spermatozoa, which stain uniformly with BSA-$DiIC_{16}$ over their entire surface, never contained particles whereas spermatozoa from the distal caput epididymidis and cauda epididymidis were similar to ejaculated spermatozoa (results not shown).

One explanation for the observed behaviour of the mobile $DiIC_{16}$ particles is that they are intracellular and represent Brownian motion in the cytoplasm. Three pieces of evidence argue against this interpretation. First, spermatozoa lack classic endoplasmic reticulum and Golgi membranes, and the only substantial cytoplasm is found in the droplet attached to the tail. This droplet usually detaches during ejaculation. Second, it is known from electron microscopic evidence that the plasma membrane and underlying outer acrosomal membrane are very closely apposed to each other, with <10 nm space between them. This is too small to accommodate the 100-400 nm diameter particles mentioned above. Third, AFM of $DiIC_{16}$-labelled spermatozoa followed by line-profile analysis revealed projections, ~200 nm in diameter, on the surface of the membrane coincident with the fluorescent particles (Fig. 3A,B). This is not compatible with the particles being intracellular. For these reasons, we consider the diffusing particles to be incorporated into the surface membrane.

Trajectory analysis of $DiIC_{16}$ particle diffusion in the plasma membrane of spermatozoa

The presence of mobile $DiIC_{16}$ particles over the acrosomal plasma membrane enabled us to investigate the molecular organisation of this region with respect to: (a) the presence of a putative diffusion barrier between the equatorial segment and

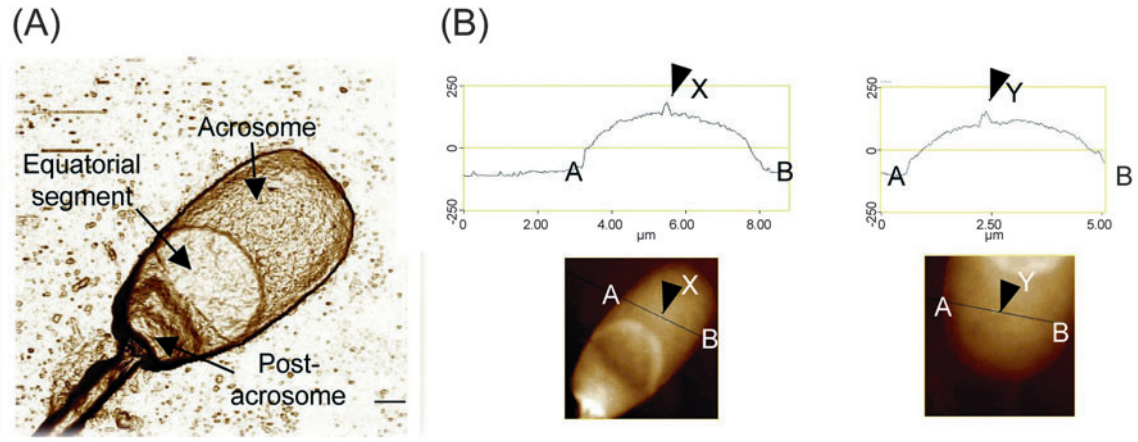

Fig. 3. AFM imaging of boar sperm heads with attached particles of $DiIC_{16}$. (A) Contact mode image to illustrate topographical features and extent of the anterior acrosome, equatorial segment and postacrosome. (B) Line-profile analysis (A-B) across two sperm heads with attached particles (labelled X and Y) on the anterior acrosomal plasma membrane. In each case a small peak, ~200 nm diameter, is coincident with the position of the $DiIC_{16}$ particle. Bars, 2 µm in A; 1 µm in B.

the anterior acrosomal plasma membrane, and between the equatorial segment and the postacrosomal plasma membrane (see Fig. 2A); (b) whether particle diffusion is random or anomalous (constrained, directed, etc.). Given their dimensions, they can be regarded as molecular aggregates or complexes, in contrast to the diffusion of individual molecules measured by FRAP and FLIP.

The strong and relatively stable fluorescence from $DiIC_{16}$ enabled the particles to be followed by epifluorescence microscopy over relatively long diffusion times (30 to 100 seconds, depending on their size) before they bleached. Of 116 mobile particles observed on 57 different spermatozoa, >95% remained within the confines of the acrosomal compartment (equatorial segment + anterior acrosomal plasma membrane) and did not invade the postacrosmal region. Diffusing particles slowed down noticeably when they approached the equatorial segment-postacrosomal boundary, frequently appearing to 'bump' against an 'obstacle' before moving away. Similarly at the edge of the sperm head, suggesting they did not pass from one face to the other. Typically, a rapidly diffusing particle traversed between the equatorial segment and the anterior acrosomal plasma membrane without any noticeable change in its speed or behaviour. Thus, although the topography of the membranes overlying these two domains is very different, as determined by AFM (Fig. 3A) (see also Ellis et al., 2002), there was no apparent change in the diffusion of $DiIC_{16}$ particles as they moved between them. Mobile particles on the postacrosomal plasma membrane were rare and, if present, moved slowly over very short distances until they bleached completely within ~20 seconds.

Confocal microscopy coupled with video recording enabled the trajectories of diffusing $DiIC_{16}$ particles to be followed in real time. Typical examples, taken from 67 particles tracked on 44 different spermatozoa in nine separate experiments, are shown in Fig. 4 and are colour-coded to enable continuous visualisation of the particle, beginning with dark blue, light blue, dark green, light green, brown and red. In four instances (Fig. 4A-C,I) the particle is shown diffusing over the anterior acrosomal plasma membrane, while in the remaining five examples (Fig. 4D-F,G) it moves between the equatorial segment and the anterior acrosomal

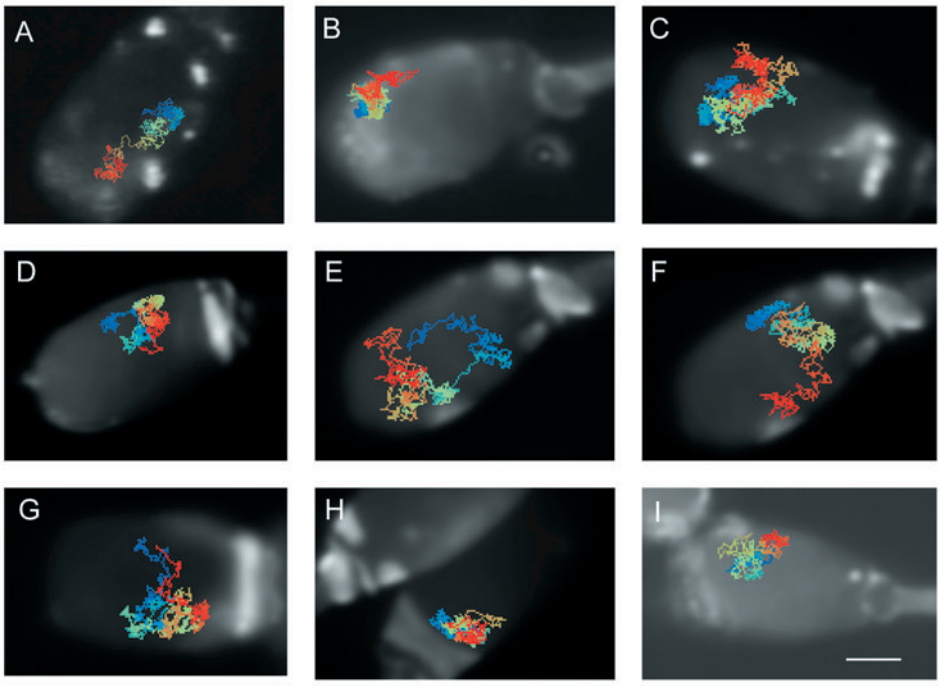

Fig. 4. Trajectories of $DiIC_{16}$ particles diffusing over the anterior acrosome and equatorial segment compartments of nine representative spermatozoa. The trajectories are colour-coded (beginning with dark blue to light blue to dark green to light green to brown to red) and change every 8 seconds. Bar, 2 µm.

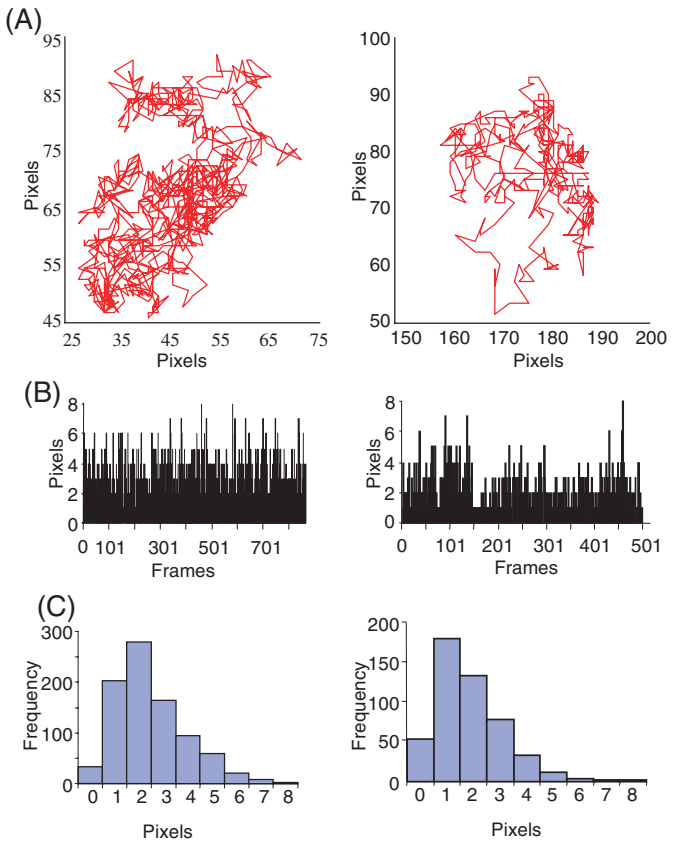

Fig. 5. (A) A detailed analysis of particle trajectories reveals jump sizes of varying lengths. Two representative examples are shown. (B) Individual jumps are plotted in sequence. (C) Frequency of jump sizes. The most frequent jump sizes are equivalent to one and two pixel points (one pixel = ~60 nm).

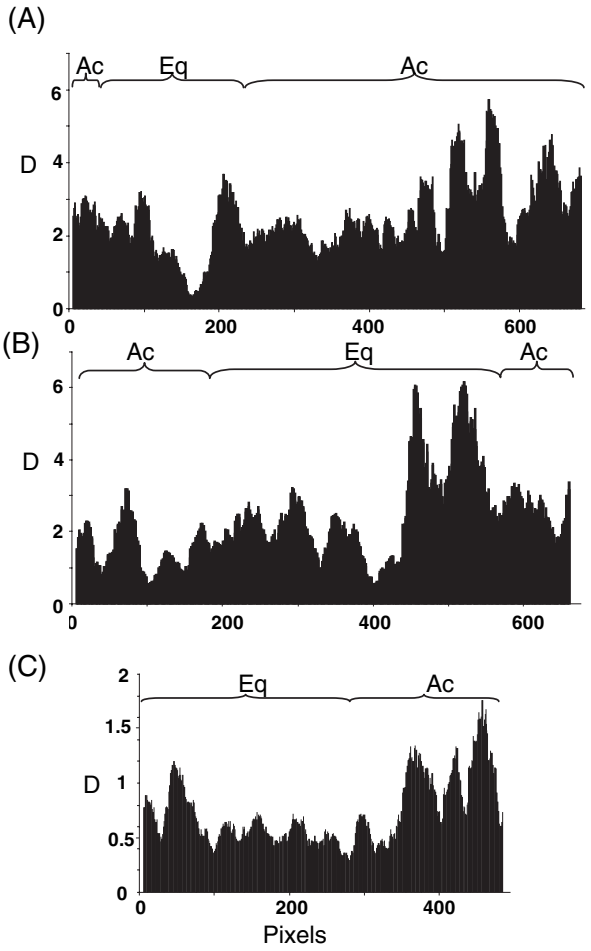

Fig. 6. Calculated D values ($\times 10^{-9}$ cm^2/second) of three representative particles diffusing between the equatorial segment and anterior acrosomal plasma membranes. An approximate periodicity is apparent irrespective of the position of the particle, but there are no consistent differences between the two compartments.

plasma membrane. When the particle reached the edge of the head or the equatorial segment-postacrosomal boundary it diffused rapidly within a small area (see dark blue trajectory in Fig. 4F,H).

More detailed analysis of this data revealed that the distance travelled by particles varied from short to long jumps (Fig. 5). At a constant camera speed (30 frames/second), six different classes were apparent. The longest jump distance (five pixels) occurred only 4% of the time, with the most frequent being one pixel (33%), two pixels (30%) and three pixels (15%) (Fig. 5C). Very occasionally (<2%), six and seven pixel jumps took place. These examples refer to the diffusion of a particle near the centre of the sperm head that crossed several times between the equatorial segment and anterior acrosomal plasma membrane. Particles diffusing close to the edge of the sperm head became constrained in one direction, as shown by a succession of very short jumps. A similar pattern was apparent when the particle was close to the junction between the equatorial segment and the postacrosomal region.

The variation in jump size was accompanied by up to tenfold fluctuations in D values. Fig. 6 shows three representative examples of particles that exchanged between the equatorial segment and anterior acrosomal plasma membrane. D values showed an approximate periodicity irrespective of the membrane compartment and there was no obvious change as the particle crossed the boundary from one compartment to another and back again (Fig. 6A,B). It was noticeable that the D values for the particles were substantially slower (eight- to 75-fold) than those measured by FRAP for single molecules of DiIC$_{16}$.

MSD analysis of DiIC$_{16}$ particle diffusion

The diffusion of a molecule or particle in a membrane may be random (Brownian motion), restricted by barriers (confined), directed (flow) or show transitions between all three modes (Saxon and Jacobson, 1997). The type of motion can frequently be identified by time-dependence plots of the MSD. MSD analysis of the nine representative examples depicted in Fig. 4 showed four plots (Fig. 7A,E,F,I) that were essentially linear with time and are characteristic of randomly diffusing particles. In five plots (Fig. 7B,C,D,G,H), however, the initially linear curves progressed towards a maximum, which may be due partly to increased error caused by the rapidly diminishing number of observations within the data-set and partly due to the particle encountering heterogeneities within the plane of the membrane. Another explanation is that as the

particle approaches the edge of the sperm head or the boundary with the equatorial segment its motion becomes restricted in either the x or y direction. This appears as transitions in the MSD plots (e.g. plot B). The motion of the particles, therefore, is essentially random, with anomalies created by edge effects and possible heterogeneities within the membrane.

Effects of cholesterol removal on diffusion of $DiIC_{16}$ particles in the plasma membrane

It is known that capacitation of spermatozoa is triggered by biochemical and organisational changes within the plasma membrane, the most important of which is a decrease in cholesterol. Capacitation is also accompanied by changes in the topographical distribution of specific membrane proteins and lipids (Jones et al., 1990; Gadella et al., 1994; Cowan et al., 2001). Exposure of boar spermatozoa to the cholesterol sequestering agent methyl-β-cyclodextrin (MBCD), for example, induces phosphorylation of specific proteins and redistribution of surface GM1 gangliosides, the latter being a useful marker for membrane rafts. Cholesterol is an important component of membrane rafts and its depletion has a significant effect on their stability, size and behaviour. It was of interest, therefore, to determine the effects of MBCD treatment on the frequency and trajectories of $DiIC_{16}$ particles in the acrosomal plasma membrane and, more importantly, whether or not it influenced the exchange of mobile particles between the equatorial segment and postacrosomal regions.

Incubating washed spermatozoa in the presence of 2.0 mmol/l MBCD in TALP medium containing 20 mmol/l bicarbonate for 1 hour before labelling with $DiIC_{16}$ caused a significant increase ($P<0.01$) in the incidence of cells with mobile particles, from ~16% in controls to ~46% ($n=4$ experiments) in treated cells. Mobile particles on MBCD-treated spermatozoa, however, still did not diffuse across the junction between the equatorial segment and the postacrosome. In addition, the trajectories, jump sizes and D values of particles were not significantly altered by MBCD treatment (results not shown).

Discussion

The results of this investigation suggest that on the sperm head there is a functional diffusion barrier to large molecular complexes between the equatorial segment and postacrosomal compartments but that individual molecules are capable of free exchange across the barrier.

A long-standing problem in membrane biology is to understand how differentiated cells such as spermatozoa maintain a polarised distribution of specific components in an essentially fluid environment. At one level these components may be confined within relatively stable compartments or macrodomains several square micrometres in area, while at another level they may be sequestered into microdomains, <50 nm in diameter, containing only several hundred molecules. Many of the mechanisms associated with maintaining lateral asymmetry in somatic cell membranes (e.g. polarised trafficking, selective internalisation) are not present in spermatozoa, which provide an excellent model for studying diffusion barriers. There is a morphological basis for them in the presence of electron-dense structures within and below the plasma membrane (e.g. the posterior ring and annulus), and AFM and FRAP studies have revealed different surface topographies and lipid diffusion dynamics between domains. Against this are reports of inter-domain migration of glycoprotein and glycolipid antigens during sperm maturation and capacitation (Cowan et al., 1987; Cowan et al., 2001; Jones et al., 1990; Gadella et al., 1994; Hunnicutt et al., 1997), suggesting that if diffusion barriers are present they are selective and dynamic as they respond to external signals. Given the current evidence for lipid rafts in cell membranes and confinement of lipids and proteins within microdomains by pickets and fences (Richie et al., 2003), it has been necessary to apply high resolution imaging techniques to follow molecular motion in the membranes of live spermatozoa.

In this investigation we have used FLIP and SPFI to assess if diffusion barriers are present at the junctional boundaries between the three different compartments on the sperm head, namely the postacrosome, equatorial segment and anterior acrosome. FLIP analysis did not provide evidence for a diffusion barrier to $DiIC_{16}$ between any of these compartments, from which it has to be concluded that lipid molecules are freely diffusing throughout the head plasma membrane. A necessary reservation here is that $DiIC_{16}$ is not a natural lipid and is not subject to

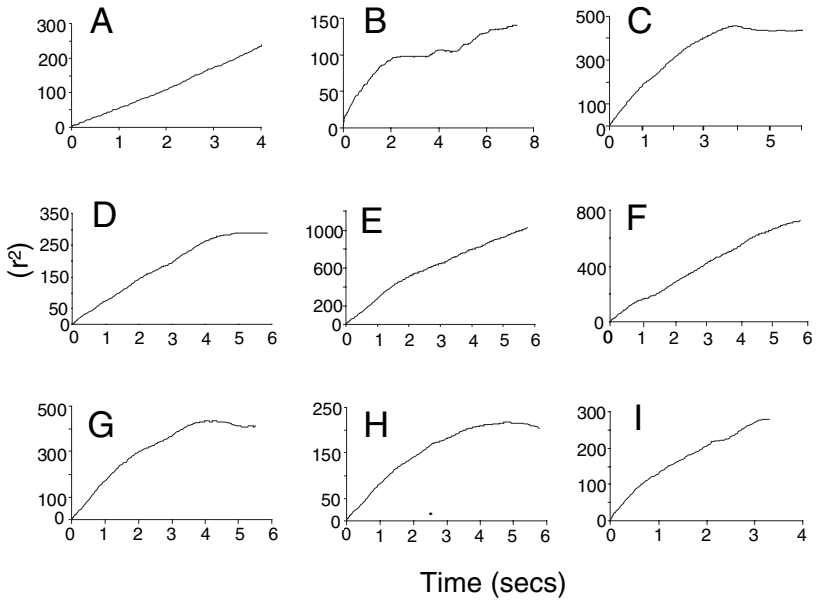

Fig. 7. Mean square displacement analysis of the nine particle trajectories (A–I) shown in Fig. 4. The essentially linear nature of the initial trajectories indicates random motion. When a particle approaches the edge of the head (as in B) or the boundary with the postacrosome (as in H), it becomes non-random due to restricted movement in the *x* or *y* axis. This coincides with a succession of short jumps before the particle moves away from the boundary.

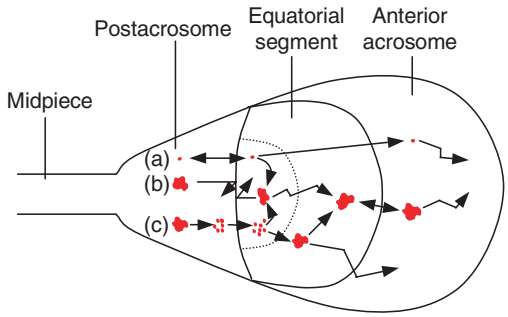

Fig. 8. Proposed model for diffusion of individual molecules versus large complexes on the sperm head. In scenario (a), a single molecule (lipid or protein) is freely diffusing between all compartments. In (b), the molecule is part of a large complex that is unable to traverse the boundary between the postacrosme and equatorial segment. This creates the impression of a barrier. In (c), the complex disassembles in the postacrosomal side of the barrier, single molecules diffuse across it and reassemble on the equatorial segment. They may reform into their original complex or join existing complexes, all of which continue to diffuse randomly.

metabolic turnover. It has also been claimed that $DiIC_{16}$ partitions preferentially into liquid ordered microdomains (Mukherjee et al., 1999). However, there was no indication of this behaviour in live boar spermatozoa, which, aside from those with attached particles, were stained uniformly throughout the head. In addition, recovery in the bleached area after FLIP was ~90%, which argues against partitioning into a pre-existing immobile phase or irreversible damage to the membrane caused by the laser beam. Thus, there are good reasons to believe that in those spermatozoa subjected to FLIP analysis, $DiIC_{16}$ behaved as a single freely diffusing molecule within the membrane.

Contrary to the above, SPFI analysis was consistent with a barrier between the equatorial segment and postacrosome. It is not clear at present whether the $DiIC_{16}$ particles formed spontaneously within the membrane or if they were taken up directly from the medium during labelling. The finding that the proportion of labelled spermatozoa with mobile particles increased with time of incubation following MBCD treatment favours the former possibility, although it could also mean that MBCD induced previously stationary particles to become mobile. MBCD at the concentrations used here induces capacitation-like changes in boar spermatozoa without significantly disturbing lipid diffusion (Shadan et al., 2004). Higher concentrations have an adverse affect, causing disruption of lipid rafts and an increase in the immobile phase. Whatever their origins, the particles remained as discrete entities within the membrane, as revealed by AFM and did not mix with the surrounding lipids, although the possibility of some dynamic exchange cannot be excluded. In one sense, the particles could be regarded as specialised lipid rafts, albeit unusual ones, because of their homogenous composition, size and apparent stability. There is some evidence that lipid rafts can diffuse as discrete entities, with half-lives of several minutes (Pralle et al., 2000), although against this is the observation that GPI anchored proteins, which are usually found in lipid rafts, do not always undergo correlated diffusion with one another (Kenworthy et al., 2004). Our finding that diffusing $DiIC_{16}$ particles remained within the confines of the anterior acrosome and equatorial segment and did not cross onto the postacrosome suggests the presence of a barrier between the latter two domains. Therefore, while individual $DiIC_{16}$ molecules are able to diffuse from the equatorial segment to the postacrosome and vice versa, large molecular complexes are unable to do so.

The precise nature of diffusion barriers in plasma membranes remains problematic, despite strong evidence for their presence in diverse cell types, ranging from chlamydomonas (Hunnicutt et al., 1990) to frog retinol rod cells (Peters et al., 1983), mammalian epithelial cells (Gumbiner and Louvard, 1985) and spermatozoa. Only recently, however, have mechanistic insights been forthcoming. From their studies on rat developing neurons, using optical tweezers and single molecule tracking experiments with Cy3-DOPE, Nakada et al. (Nakada et al., 2003) have provided evidence for a diffusion barrier in the initial segment region between the cell body and axon, and proposed a model in which a localised concentration of transmembrane proteins anchored to the cytoskeleton impede lipid and protein diffusion through a combination of steric hindrance and hydrodynamic drag. Obvious candidates for picket proteins are ion channels, which do not diffuse laterally, or at best only very slowly, because of their attachment to the membrane skeleton. Supporting this view is a concentration of sodium channels and ankryin in the initial segment and the prediction from Monte Carlo modelling studies that, for as little as a 10% increase in coverage by anchored picket proteins, diffusion rates decrease approximately 100-fold (Nakada et al., 2003). This prediction is potentially of great significance, as it suggests a means by which cytoskeletal-induced changes in the number and disposition of transmembrane proteins could have disproportionate influences on barrier function, and hence surface compartmentalisation. On spermatozoa, many equatorial segment-specific antigens have been described (Allen and Green, 1995), among which may be mentioned voltage-gated Ca^{2+} channels (Benhoff, 1999), calmodulin (Camatini and Casale, 1987), actin and thymosin β-10 (Howes et al., 2001). Thus, together with the present data and the topographical appearance revealed by AFM, there is circumstantial evidence for the presence of anchored transmembrane proteins in the equatorial segment. Lateral heterogeneity on the nanometre scale is also present within the equatorial segment itself, in the form of an unusual area termed the ‘subsegment’ (Ellis et al., 2002) and a diffuse layer rich in cholesterol that lies immediately below the separating boundary with the postacrosome (P.S.J. and R.J., unpublished). Given that the proportion of cholesterol has a profound effect on miscibility of bilayer lipids (Lawrence et al., 2003), and a reduction in membrane cholesterol is a key step in sperm capacitation (Cross, 1998; Travis and Kopf, 2002), there are good reasons for thinking that the interface between the equatorial segment and postacrosome is an important site for regulation of exchange of membrane components between compartments. Very high resolution techniques involving single molecule tracking of raft and non-raft components will have to be applied to further assess the veracity of this hypothesis.

Diffusion of $DiIC_{16}$ particles within the equatorial segment and anterior acrosomal domains was random, except when

the particle approached the edge of the head or the boundary with the postacrosome. One explanation for the variation in jump size and D values is that they reflect heterogeneities or obstacles encountered by the particles as they diffuse through the membrane. It is not known if microdomains of the kind envisaged by Kusumi and co-workers (Richie et al., 2003) are present in sperm plasma membranes or not, as single molecule tracking experiments have not yet been applied to this cell. Nor is it generally known what proportion of a cell membrane consists of rafts under steady state conditions. On the basis of extensive FRAP analysis of COS-7 cells, Kenworthy et al. (Kenworthy et al., 2004) were unable to distinguish between a dynamic partitioning model, in which membrane components exchanged rapidly between raft and non-raft regions, and a no raft model. In the case of boar spermatozoa, lipid rafts have been isolated biochemically from non-capacitated cells and, as visualised by cholera toxin (CTXB) for GM1 gangliosides, are distributed mainly over the sperm tail (Shadan et al., 2004). A reduction of cholesterol levels with MBCD to induce capacitation, however, results in CTXB binding to the acrosomal domain with concomitant loss from the tail, implying that rafts either migrate in an anterior direction as discrete entities or there is a process of disassembly and migration as single molecules, followed by reassembly. The current results favour the latter possibility with the disassembly-reassembly processes taking place at the junction between the postacrosome and equatorial segment. Once on the acrosomal domain, the reassembled complexes would be freely diffusing but unable to pass back through the barrier. In this hypothesis (Fig. 8) the barrier acts like a selective 'filter' to allow exchange of individual lipid or protein molecules but not complexes of even a few tens of molecules. Because the complexes are freely diffusing, they would have high D values in conventional FRAP experiments. The model also implies directionality by the barrier transport mechanisms to enable accumulation of specific molecules on one side. This may be a property of the molecules in question, as it is noteworthy that those glycoproteins that migrate have GPI anchors (Cowan et al., 1987; Jones et al., 1990) and would be predicted to be sequestered preferentially into lipid rafts. The stability and dynamics of lipid rafts in sperm membranes, therefore, seems to be central to many developmental processes, such as maturation and capacitation, and explains why lowering cholesterol levels triggers intracellular signalling events, leading to acquisition of fertilizing capacity (Cross, 2004).

In conclusion, the data presented here offer an explanation for compartmentalisation of the sperm head while permitting the polarised migration of specific glycoproteins and glycosphingolipids. Important questions to be answered in future work are the mechanisms for disassembly-reassembly of protein and lipid complexes at the equatorial segment barrier, the physical basis for such a barrier and the role of the membrane cytoskeleton.

This work was supported by the BBSRC and a Junior Research Fellowship from Emmanual College, University of Cambridge UK, to one of us (T.B.). We thank Dr Robert Henderson, Department of Pharmacology, University of Cambridge UK, for use of the AFM, and staff at JSR Newsham UK for provision of boar semen.

References

Allen, C. A. and Green, D. P. (1995). Monoclonal antibodies which recognise equatorial segment epitopes presented de novo following the A23187-induced acrosome reaction of guinea pig sperm. *J. Cell Sci.* **108**, 767-777.

Anderson, C. M., Georgiou, G. N., Morrison, I. E. G., Stevenson, G. V. W. and Cherry, R. J. (1992). Tracking of cell surface receptors by fluorescent digital imaging microscopy using a charge-coupled device camera: low intensity lipoprotein and influenza virus receptor mobility at 4°C. *J. Cell Sci.* **101**, 415-425.

Benhoff, S. (1999). Receptors and channels regulating acrosome reactions. *Hum. Fertil.* **2**, 42-55.

Camatini, M. and Casale, A. (1987). Actin and calmodulin coexist in the equatorial segment of ejaculated boar sperm. *Gamete Res.* **17**, 97-105.

Cardullo, R. A. and Wolf, D. E. (1990). The sperm plasma membrane. A little more than mosaic, a little less than fluid. In *Ciliary and Flagellar Membranes* (ed. R. A. Bloodgood), pp 305-336. New York, NY: Plenum Press.

Cowan, A. E., Myles, D. G. and Koppel, D. E. (1987). Lateral diffusion of the PH-20 protein on guinea pig sperm: evidence that barriers to diffusion maintain plasma membrane domains in mammalian sperm. *J. Cell Biol.* **104**, 917-923.

Cowan, A. E., Myles, D. G. and Koppel, D. E. (1991). Migration of the guinea pig sperm membrane protein PH-20 from one localized surface domain to another does not occur by a simple diffusion trapping mechanism. *Dev. Biol.* **144**, 189-198.

Cowan, A. E., Koppel, D. E., Vargas, L. A. and Hunnicutt, G. R. (2001). Guinea pig fertilin exhibits restricted lateral mobility in epididymal sperm and becomes freely diffusing during capacitation. *Dev. Biol.* **236**, 502-509.

Cross, N. L. (1998). Role of cholesterol in sperm capacitation. *Biol. Reprod.* **59**, 7-11.

Cross, N. L. (2004). Reorganization of lipid rafts during capacitation of human sperm. *Biol. Reprod.* **71**, 1367-1373.

Dragsten, P. R., Blumenthal, R. and Handler, J. S. (1981). Membrane asymmetry in epithelia: is the tight junction a barrier to diffusion in the plasma membrane? *Nature* **294**, 718-722.

Edidin, M. (1993). Patches and fences: probing for plasma membrane domains. *J. Cell Sci.* **7**, 165-169.

Edidin, M. (2003). The state of lipid rafts: from model membranes to cells. *Annu. Rev. Biophys. Biomol. Struct.* **32**, 257-283.

Ellis, D. J., Shadan, S., James, P. S., Henderson, R. M., Edwardson, J. M., Hutchings, A. and Jones, R. (2002). Post-testicular development of a novel membrane substructure within the equatorial segment of ram, bull, boar and goat spermatozoa as viewed by atomic force microscopy. *J. Struct. Biol.* **138**, 187-198.

Fujiwara, T., Richie, K., Murakoshi, H., Jacobson, K. and Kusumi, A. (2002). Phospholipids undergo hop diffusion in compartmentalized cell membranes. *J. Cell Biol.* **157**, 1071-1081.

Gadella, B. M., Gadella, T. W., Jr, Colenbrander, B., van Golde, L. M. G. and Lopez-Cardoyo, M. (1994). Visualization and quantitation of glycolipid polarity dynamics in the plasma membrane of the mammalian spermatozoon. *J. Cell Sci.* **107**, 2151-2163.

Gumbiner, B. and Louvard, D. (1985). Localized barriers in the plasma membrane: a common way to form domains. *Trends Biochem. Sci.* **10**, 435-438.

Holt, W. V. (1984). Membrane heterogeneity in the mammalian spermatozoon. *Int. Rev. Cytol.* **87**, 159-194.

Howes, E. A., Hurst, S. M. and Jones, R. (2001). Actin and actin-binding proteins in bovine spermatozoa: potential role in membrane remodelling and intracellular signalling during epididymal maturation and the acrosome reaction. *J. Androl.* **22**, 62-72.

Hunnicutt, G. R., Kosfiszer, M. G. and Snell, W. J. (1990). Cell body and flagellar agglutinins in *Chlamydomonas reinhardtii*: the cell body plasma membrane is a revervoir for agglutinins whose migration to the flagella is regulated by a functional barrier. *J. Cell Biol.* **111**, 1605-1616.

Hunnicutt, G. R., Koppel, D. E. and Myles, D. G. (1997). Analysis of the process of localization of fertilin to the sperm posterior head plasma membrane domain during sperm maturation in the epididymis. *Dev. Biol.* **191**, 146-159.

Jacobson, K., Sheets, E. D. and Simson, R. (1995). Revisiting the fluid mosaic model of membranes. *Science* **268**, 1441-1442.

Jones, R., Shalgi, R., Hoyland, J. and Phillips, D. M. (1990). Topographical rearrangement of a plasma membrane antigen during capacitation of rat spermatozoa in vitro. *Dev. Biol.* **139**, 349-362.

Kahn, Z., Balch, T. and Dellaert, F. (2004). An MCMC-based particle filter

for tracking multiple interacting targets. *Euro. Confer. Comp. Vis.* **4**, 279-290.

Kalman, R. E. (1960). A new approach to linear filtering and prediction problems. *Trans. A.S.M.E. J. Basic Engineer. Series D*, **82**, 35-45.

Kenworthy, A. K., Nichols, B. J., Remmert, C. L., Hendrix, G. M., Kumar, M., Zimmerberg, J. and Lippincott-Schwartz, J. (2004). Dynamics of putative raft-associated proteins at the cell surface. *J. Cell Biol*. **165**, 735-746.

Kobayashi, T., Storrie, B., Simons, K. and Dotti, C. G. (1992). A functional barrier to movement of lipids in polarized neurons. *Nature* **359**, 647-650.

Ladha, S., James, P. S., Clark, D. C., Howes, E. A. and Jones, R. (1997). Lateral diffusion of plasma membrane lipids in bull spermatozoa: heterogeneity between surface domains and rigidification following cell death. *J. Cell Sci*. **110**, 1041-1050.

Lawrence, J. C., Saslowsky, D. E., Edwardson, J. M. and Henderson, R. M. (2003). Real-time analysis of the effects of cholesterol on lipid raft behavior using atomic force microscopy. *Biophys. J*. **84**, 1827-1832.

Mackie, A. R., James, P. S., Ladha, S. and Jones, R. (2001). Diffusion barriers in ram and boar sperm plasma membranes: directionality of lipid diffusion across the posterior ring. *Biol. Reprod*. **64**, 113-119.

Mukkerjee, S., Soe, T. T. and Marfield, F. R. (1999). Endocytic sorting of lipid analogues differing solely in the chemistry of their hydrophobic tails. *J. Cell Biol.* **144**, 1271-1284.

Murase, K., Fujiwara, T., Umemura, Y., Suzuki, K., Iino, R., Yamashita, H., Saito, M., Murakoshi, H., Richie, K. and Kusumi, A. (2004). Ultra fine membrane compartments for molecular diffusion as revealed by single molecule techniques. *Biophys. J.* **86**, 4075-4093.

Nakada, C., Richie, K., Oba, Y., Nakamura, M., Hotta, Y., Iino, R., Kasai, R. S., Yamaguchi, K., Fujiwara, T. and Kusumi, A. (2003). Accumulation of anchored proteins forms membrane diffusion barriers during neuronal polarization. *Nat. Cell Biol*. **5**, 626-633.

Parrish, J. J., Susko-Parrish, J., Winer, M. A. and First, N. L. (1988). Capacitation of bovine sperm by heparin. *Biol. Reprod*. **38**, 1171-1180.

Peters, K. R., Palade, G. E., Schmeider, B. G. and Papermaster, D. S. (1983). Fine structure of a periciliary ridge complex of frog retinol rod cells revealed by ultrahigh resolution scanning electron microscopy. *J. Cell Biol*. **96**, 265-276.

Pralle, A., Keller, P., Florin, E.-L., Simons, K. and Horber, J. K. H. (2000). Sphingolipid-cholesterol rafts diffuse as small entities in the plasma membrane of mammalian cells. *J. Cell Biol.* **148**, 979-1007.

Primakoff, P. and Myles, D. G. (1983). A map of the guinea pig sperm surface constructed with monoclonal antibodies. *Dev. Biol*. **98**, 417-428.

Richie, K., Iino, R., Fujiwara, T., Murase, K. and Kusumi, A. (2003). The fence and picket structure of the plasma membrane of live cells as revealed by single molecule techniques. *Mol. Membr. Biol*. **20**, 13-18.

Rodriguez-Boulan, E. and Nelson, W. J. (1989). Morphogenesis of the polarized epithelial cell phenotype. *Science* **245**, 718-725.

Saxton, M. J. and Jacobson, K. (1997). Single particle tracking: applications to membrane dynamics. *Annu. Rev. Biophys. Biomol. Struct.* **26**, 373-399.

Shadan, S., James, P. S., Howes, E. A. and Jones, R. (2004). Cholesterol efflux alters lipid raft stability and distribution during capacitation of boar spermatozoa. *Biol. Reprod*. **71**, 253-265.

Travis, A. J. and Kopf, G. S. (2002). The role of cholesterol efflux in regulating the fertilization potential of mammalian spermatozoa. *J. Clin. Invest*. **110**, 731-736.

Van Drogen, F. and Peter, M. (2004). Revealing proteins dynamics by photobleaching techniques. *Methods Mol. Biol*. **284**, 287-306.

Vereb, G., Szollosi, J., Matko, J., Nagy, P., Farkas, T., Vigh, L., Matyus, L., Waldman, T. A. and Damjanovich, S. (2003). Dynamic yet structured: the cell membrane three decades after the Singer-Nicolson model. *Proc. Natl. Acad. Sci. USA* **100**, 8053-8058.

Wolf, D. E. (1995). Lipid domains in sperm plasma membranes. *Mol. Membr. Biol.* **12**, 101-104.

Wolfe, C. A., James, P. S., Mackie, A. R., Ladha, S. and Jones, R. (1998). Regionalized lipid diffusion in the plasma membrane of mammalian spermatozoa. *Biol. Reprod*. **59**, 1506-1514.